Journal on Applied and Chemical Physics

Vol: 2(4), December 2023

REST Publisher; ISSN: 2583-7125

Website: https://restpublisher.com/journals/jacp/

DOI: https://doi.org/10.46632/jacp/2/4/4

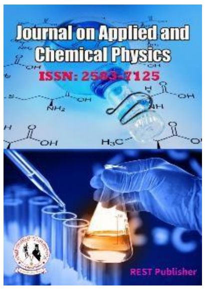

Orthopedic Calcium Hydrogen Phosphate Corrosion Behavior in Surgical 316L Stainless Steel Composites

***Chandrasekar Raja, M. Ramachandran, Vidhya Prasanth, Prabakaran Nanjundan**

REST Labs, Kaveripattinam, Krishnagiri, Tamil Nadu, India.

*Corresponding Author Email: chandrasekarrajarsri@gmail.com

Abstract: *Porosity biomedical implants are recognized for their enhanced Osseo integration due to bone tissue growth, along with an elastic modulus that is lower for stiff implants, causing stress retention and a lower likelihood of implant loosening. The implant's moist ability is critical for optimal tissue-implant integration and is highly dependent on the material's surface topography. Recent research has revealed that plastic bending processes can improve cell response while also increasing the roughness of the surface and strength. The electrochemical behavior of a 316L Surgical stainless steel alloy (316L SS) bone implant in Hank's solution (pH 7.4) at 37 °C with along with with varying concentrations of calcium hydrogen phosphate was examined. This drug acts as an inhibitor, protecting the surface of the composite from the corrosive physiologic media. The results show that a medication concentration of 113 M is quite safe for 316L stainless steel bone implants. To monitor 1 mm Alendronate sodium (ALN) medication, a low-cost and easily produced 316L stainless steel alloys altered Orthopedic Calcium Hydrogen Phosphate was built. In simulated physiological fluid (pH 7.4), the corrosion-resistant capabilities of a surgical 316 L Surgical Steel (SS) bone implant coated with a novel Orthopedic Calcium Hydrogen Phosphate coating were investigated. The overall Cronbach's Alpha score for the model is 0.505 when using the statistical software SPSS version 16.*

Keywords: *Hanks' solution, surgical 316L Stainless Steel, Electrochemical Impedance Spectroscopy.*

1. INTRODUCTION

In the medical implant industry, stainless steel is the most widely utilized material, “particularly in the manufacture of orthopedic implants and a variety of other biomedical devices such as shattered bones, fixtures, dental posts, and screws” [1]. Because of its acceptable biocompatibility, strong corrosion resistance, and inexpensive cost, 316L stainless steel alloy (316L SS) has been frequently employed as a medical implant [2]. “Its key benefits include biocompatibility, good mechanical qualities related to bone minerals, corrosion resistance, ease of fabrication, and low cost [5]. Calcium hydrogen phosphate (CHP) has been utilized as a bone supplement in combination with other substances [2-4]”. Because of their low cost, simplicity, and broad applicability, electrochemical sensors are valuable instruments. “Carbon paste electrode (CPE) is employed for material determination due to its inert electrochemistry, easily regenerated changed surface, and low cost. Chemically modified electrodes provide a lower detection limit while increasing sensitivity [13-16]”. Silver nanoparticles (AgNPs) are inexpensive and extremely conductive, making them ideal for biosensing applications. Chitosan (CS) [1] is a polysaccharide that is commonly utilized in bio-modification. Because of its unique both chemical and physical qualities, as well as its wide surface area, cellulose phthalate has applications [16-19]. Sivaraj and Kwijayalakshmi [6] investigated SS alloys with an implant made of a new bioactive hydroxyapatite/F-multiwalled carbon nanotube composite. “Fekri and Assab [15] investigated 316L SS alloy as an ibandronate surgical implant. The resistance to corrosion of Ce-doped niobium oxide-coated 316L SS with orthopedic applications is investigated by Khata and Nallian [7]. The purpose of this research is to investigate the corrosion reaction of the 316L stainless steel in Hank's solution (pH 7.4) at 37 °C without and with various concentrations of CHP bone medication as an inhibitor for safeguarding the composite surface from the surrounding corrosive biological surface. Furthermore, for drug testing and corrosion monitoring, a novel, simple, and low-cost ACCMCPE sensors based on carbon paste (CP) coated with chitosan (CS), cellulose (CE), and silver nanoparticles (AgNPs) have been produced”. Hank's solution:“Hanks' solution [13, 14] is used as the test solution, and it contains (g/l) NaCl: 8.74, $NaHCO_3$: 0.35, Na_2HPO_4: 0.06 and NaH_2PO_4: 0.06 (Analar grade reagents). The orthopedic drug CHP (SigmaAldrich) is employed. All solutions were created. An EC-Lab SP 150 Potentiostat electrochemical workstation was used for all voltammetry studies. At a scan rate of 1 mV/s, potentiodynamic polarization tests were carried out. EIS studies are carried out at amplitudes of 10 mV and frequencies ranging from 0.1 Hz to 100 kHz. To corroborate the results, each experiment has been carried out and repeated between two and three times at 37°C. SEM model Quanta 250 FEG (Field Emission Gun) and attached to EDX unit (Energy Dispersive X-ray Analysis), voltage 30 K.V., magnifying 14up, resolution up to10, 00,00, for Gun1n (FEI Institute, The Netherlands) were used to examine the surface morphologies of the materials". SPSS (Statistical Package for the Social Sciences) is a program that is used by academics in a variety of areas for quantita-tive data analysis. SPSS provides descriptive and bivariate statistics, numeric effect projections, and group identification predictions for data analysis. The software also has data conversion, mapping process, and direct marketing capabilities. The software interface displays publicly accessible information in its main view, similar to a spreadsheet. This paper was analyzed using SPSS version 16.

2. ANALYSIS AND DISCUSSION

Measurements with Electrochemical Impedance Spectroscopy (EIS):"The Bode graphs for surgical 316L SS alloy metal submerged in Hanks' solution at pH 7.4 and 37 °C for 0, 1, 4, 5, and 7 days with and without varied doses of calcium hydrogen phosphate (CHP) medicine (1×10^{-3} M, 1×10^{-4} M and 1×10^{-5} M)". It was revealed that increasing the immersion time as well as the concentration of CHP medicine raises the impedance (Z) values. The compound may be absorbed through those pairs of electrons on the surface since this medication has a pair of protons on the oxygen atom. Furthermore, the development of an anti-Ca-P barrier by the production of a well-protected film is caused by the Coulombic force acting on these single pairs of oxygen or phosphorus atoms. This adsorbed layer thickens as the medication concentration or immersion time increases, acting as a corrosion preventative.

TABLE 1. EIS parameters for surgical 316L SS alloy in Hanks' solution were investigated at 37 °C without and with various CHP concentrations.

Conc. (M)	R_s (Ω/cm)	R1 (KΩ/cm^2)	Q1 (μF/cm^2)	n1	R2 (KΩ/cm^2)	Q2 (μF/cm^2)	n2	IE%
0(1 h)	50.12	0.194	5.13	0.69	0.451	0.91	0.83	0
0(1 day)	48.97	0.299	5.42	0.69	1.500	0.86	0.85	0
0(4 days)	48.88	0.834	4.77	0.78	1.161	0.82	0.85	0
0(5 days)	48.69	0.971	4.12	0.79	1.203	0.78	0.87	0
0(7 days)	20.93	1.829	4.06	0.84	3.183	0.61	0.89	0
1×10^{-5} (1 h)	6.309	0.315	4.14	0.80	2.197	0.74	0.93	74.32
1×10^{-5}(1 day)	13.45	0.338	4.10	0.81	2.210	0.72	0.96	29.40
1×10^{-5}(4days)	63.11	0.936	4.07	0.81	2.612	0.68	0.99	43.77
1×10^{-5}(5 days)	70.79	0.987	4.03	0.82	3.021	0.59	0.95	45.76
1×10^{-5}(7 days)	72.45	1.3530	3.97	0.85	199.005	0.24	0.98	97.64
1×10^{-4} (1 h)	8.04	0.359	4.02	0.89	3.356	0.58	0.94	82.64
1×10^{-4} 1 day)	14.19	0.989	3.91	0.88	4.023	0.55	0.95	64.11
1×10^{-4}(4 days)	16.97	2.784	2.98	0.89	5.163	0.51	0.97	74.90
1×10^{-4}(5 days)	66.07	3.192	2.19	0.93	6.211	0.52	0.94	76.88
1×10^{-4}(7 days)	74.84	17.934	1.78	0.94	298.293	0.33	0.97	98.42
1×10^{-3}(1 h)	10.21	0.561	3.09	0.91	5.758	0.51	0.94	89.79
1×10^{-3} (1 day)	26.12	3.023	2.82	0.90	6.004	0.49	0.95	80.07
1×10^{-3}(4 days)	16.98	4.121	2.10	0.91	10.112	0.38	0.97	85.98
1×10^{-3}(5 days)	83.17	5.021	2.09	0.92	12.302	0.34	0.97	87.45
1×10^{-3}(7 days)	90.36	21.453	1.002	0.94	479.734	0.16	0.99	99.00

As illustrated in Figure 1f, Curves are simulated using a data-adapted two-mode constant model[1, 8-10]. Rs represents the solution resistance, whereas R1 and R2 represent the surface and interior layers, respectively. Table 1 contains relevant EIS data. Constant-phase element (CPE) capacitors are used as a better capacitance alternative due to surface variability [11, 12]. The inhibitory efficiency (IE%) of calcium hydrogen phosphate as a blocking agent is computed by using the following solution [46] and is provided in Table 1:

$$IE\% = \frac{RT - RT}{RT} \text{ ---------------- } (1)$$

The total resistance for 316L SS metals without and/or with inhibitors is expressed as RoT and RT. The results show that increasing the calcium hydrogen phosphate concentration improves the general resistance and IE% of the investigated electrodes. The surface effect of both absorption and the creation of films reduce the effective area, and an inhibitor concentration of 113 M raises the inhibition efficiency to 99.0%.

Corrosion Sensor Measurements: "A unique electrochemical Silver nanoparticles/chitosan/cellulose acetate phthalate modified carbon paste electrode (ACCMCPE) sensor is utilized to evaluate the corrosion behavior of 316L SS in Hank's solution (103 M) at 37 °C". As the concentration of medication grows after absorption in 316L SS alloy, it gives a peak value at the moment to check the sensor works properly. The medication concentration in Hanks' solution drops with time due to the decrease in peak current caused by infusion. Over time, when the medication adsorbs to the alloy surface, the amount presents in the hanks decreases, resulting in a fall in peak current. As a result, as an implant, this sensor can be utilized for corrosion monitoring of a 316L stainless steel alloy.

TABLE 2. Statistics on Reliability

Cronbach's Alpha	N of Items
0.505	8

Statistics on Reliability is shown in Table 2. Cronbach's Alpha for the model as a whole is 0.505, and Cronbach's alpha for standardized items is 0.505, indicating 50% dependability. Based on the literature review, models with Cronbach's Alpha values greater than 50% can be evaluated for analysis.

TABLE 3. Descriptive Statistics

	N	Range	Mean	Std. Deviation	Variance	Skewness
Rs (Ω/cm)	20	84	42.53	28.162	793.104	.170
R1 (KΩ/cm2)	20	21	3.37	5.776	33.357	2.655
Q1 (µF/cm2)	20	4	3.49	1.180	1.392	-.469
n1	20	0	.85	.075	.006	-.801
R2 (KΩ/cm2)	20	479	52.37	126.558	1.602E4	2.716
Q2 (µF/cm2)	20	1	.57	.207	.043	-.204
n2	20	0	.93	.049	.002	-1.009
IE%	20	99	56.51	38.067	1.449E3	-.595

Table 3 displays R_s (Ω/cm), R1 (KΩ/cm2), Q1 (µF/cm2), n1, R2 (KΩ/cm2), Q2 (µF/cm2), n2, IE%, Descriptive Statistical Analysis N, Range, Mean, Standard Deviation values are given.

TABLE 4. Statistics

		R_s (Ω/cm)	R1 (KΩ/cm^2)	Q1 (µF/cm^2)	n1	R2 (KΩ/cm^2)	Q2 (µF/cm^2)	n2	IE%
N	Valid	20	20	20	20	20	20	20	20
	Missing	0	0	0	0	0	0	0	0
Mode		6^a	0^a	1^a	1^a	0^a	1	1	0
Range		84	21	4	0	479	1	0	99
Minimum		6	0	1	1	0	0	1	0
Maximum		90	21	5	1	480	1	1	99
Percentiles	25	14.88	.41	2.35	.80	2.20	.41	.90	7.35
	50	48.78	.99	4.00	.86	3.69	.56	.95	74.61
	75	69.61	3.15	4.12	.91	9.14	.74	.97	87.08
a. Multiple modes exist. The smallest value is shown									

Table 4 Rs (Ω/cm), R1 (KΩ/cm2), Q1 (µF/cm2), n1, R2 (KΩ/cm2), Q2 (µF/cm2), n2, IE%, Descriptive Statistical Analysis N Valid, N Missing, Mode, Range, Minimum, Maximum, Percentiles values25, 50, 75 are given.

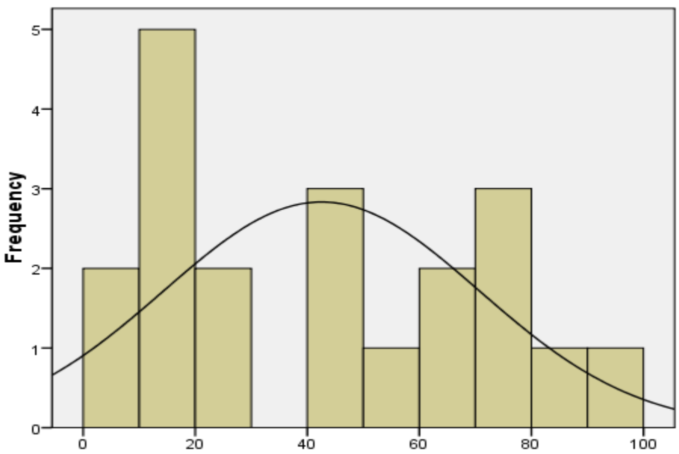

FIGURE 1. Frequency for R_s (Ω/cm) frequency

Figure 1 depicts the histogram plot for R_s (Ω /cm) frequency. It is clear from the figure that the data are slightly left skewed due to more respondents selecting 0-20 for R_s (Ω /cm) frequency. Except for the 0-20 value, all other values are under the normal curve, indicating that the model is significantly following normal distribution.

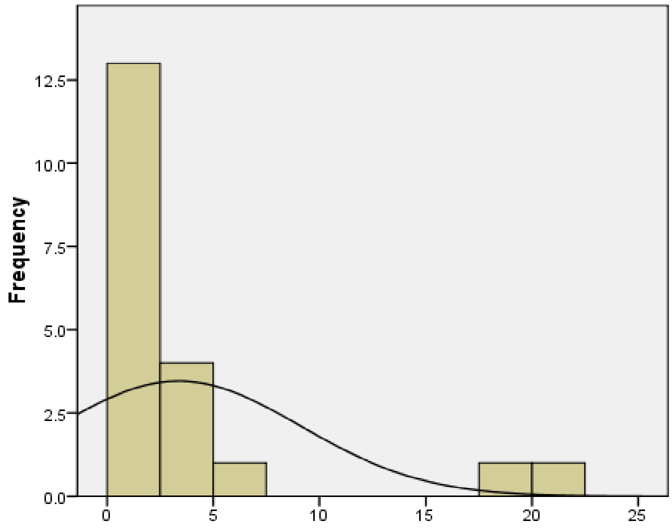

FIGURE 2. Frequency for R_1 (KΩ/cm2)

Figure 2 shows the histogram plot for R1 (KΩ/cm2) frequency. It is obvious from the image that the data are slightly left skewed due to more respondents choosing 0-5.

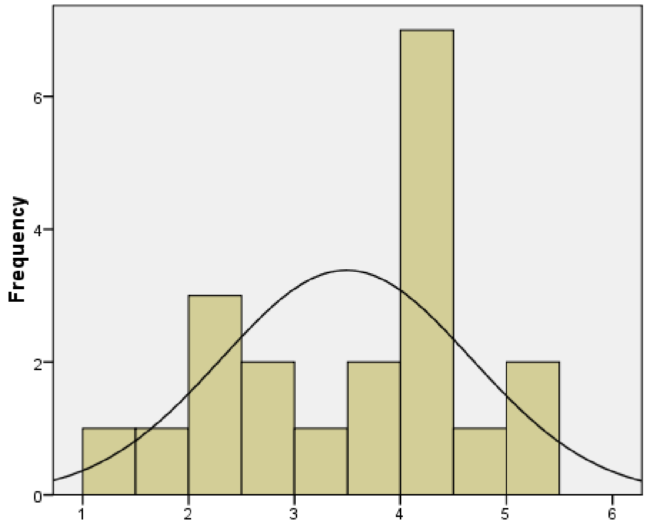

FIGURE 3. Frequency for Q1 (μF/cm2)

Figure 3 depicts the histogram plot for Q1 (μF /cm2) frequency. It is obvious from the figure that the data where all other values are beneath the normal curve, indicating that the model is strongly following a a normal distribution. However, 4-5 values provide a better reaction.

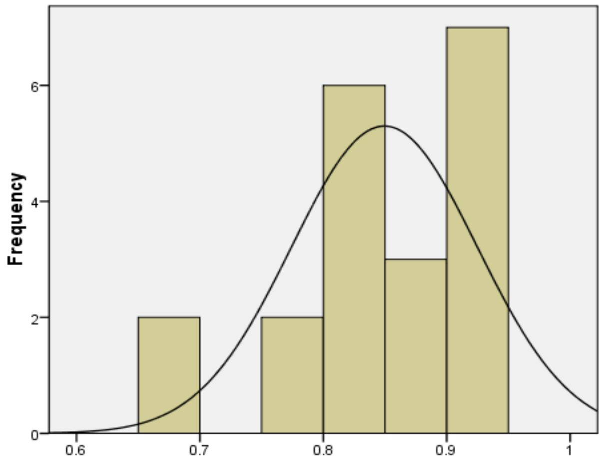

FIGURE 4. Frequency for n1

Figure 4 shows a histogram chart for n1 frequency. From the figure, it is clear that the data have slightly Wright's skewed because more respondents chose 0.9-1 for n1 frequency. Except for the 0.9-1 value, every other number falls within the normal curve, indicating that the model is significantly adhering to the normal distribution.

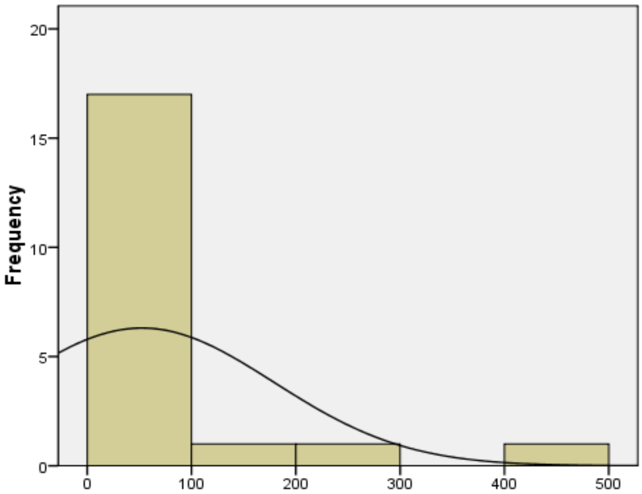

FIGURE 5. Frequency for R2 (KΩ/cm2)

Figure 5 depicts the histogram plot for R2 (KΩ /cm2) frequency. It is clear from the figure that the data are slightly left biased due to more respondents choosing 0-100 for R2 (KΩ /cm2) frequency. Except for the 0-100 value, some values are under the curve, indicating that the model is substantially following out of distribution.

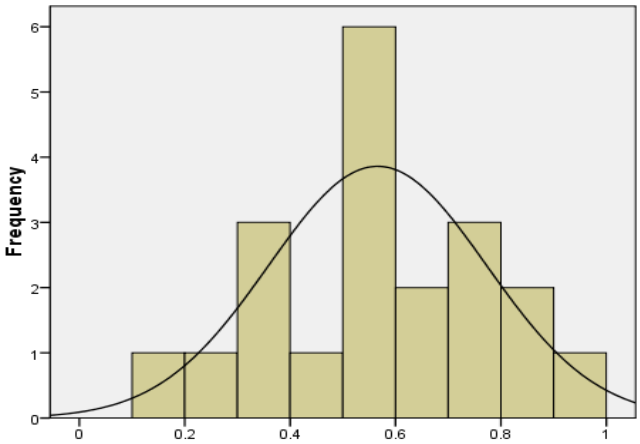

FIGURE 6. Frequency for Q2 (μF/cm^2)

Figure 6 depicts the histogram plot for Q1 (μF /cm2) frequency. It is obvious from the figure that the data where all other values are beneath the normal curve, indicates that the model is strongly following a normal distribution. However, 0.5-0.6

levels produce more responses.

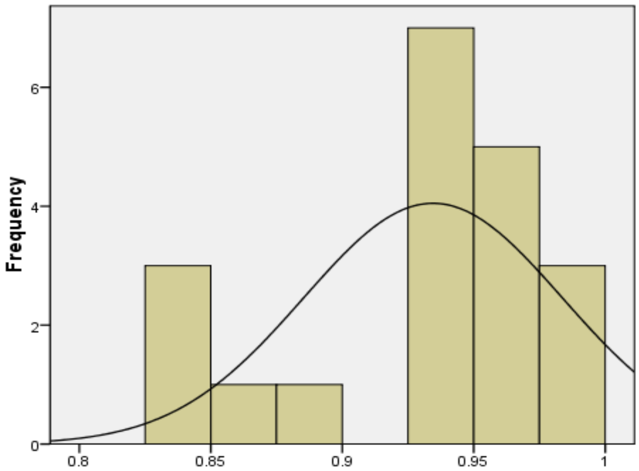

FIGURE 7. Frequency for n2

Figure 7 depicts a histogram graph for n2 frequency. It is obvious from the chart that the data are somewhat Wright-skewed due to more respondents 0.925-0.975.

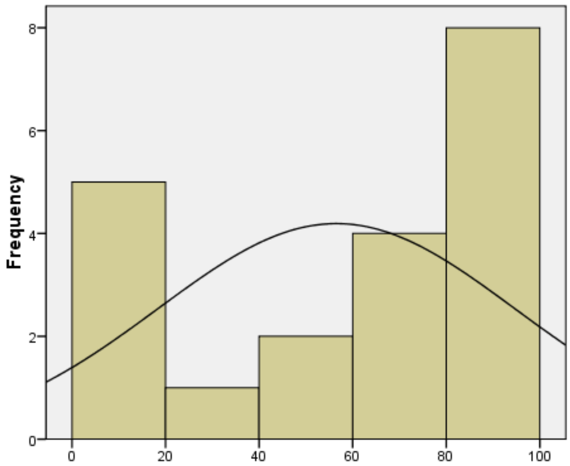

FIGURE 8. Frequency for IE%

Figure 8 depicts the histogram plot for IE% frequency. It is obvious from the figure that the numbers are slightly Wright skewed since there is more respondents 80-100 for IE% frequencies except the 0-100 values some values are the normal curve showing model is largely following normal distribution.

Table 5. Matrix of Inter-Item Correlations

	R_s (Ω/cm)	R1 (KΩ/cm^2)	Q1 (µF/cm^2)	n1	R2 (KΩ/cm^2)	Q2 (µF/cm^2)	n2	IE%
Rs (Ω/cm)	1.000	.531	-.308	.071	.565	-.354	.135	.091
R1 (KΩ/cm2)	.531	1.000	-.759	.540	.904	-.660	.409	.469
Q1 (µF/cm2)	-.308	-.759	1.000	-.893	-.578	.841	-.688	-.762
n1	.071	.540	-.893	1.000	.402	-.849	.759	.833
R2 (KΩ/cm2)	.565	.904	-.578	.402	1.000	-.671	.399	.458
Q2 (µF/cm2)	-.354	-.660	.841	-.849	-.671	1.000	-.788	-.844
n2	.135	.409	-.688	.759	.399	-.788	1.000	.825
IE%	.091	.469	-.762	.833	.458	-.844	.825	1.000

Table 4 is an inter-item relationship matrix that demonstrates the correlation coefficients between several variables. The coefficient of correlation between two variables is represented by each cell in the matrix. The coefficient of correlation is a statistical significance indicator that is used to measure the amount and direction of a relationship between two variables. It has a value between -1 and 1, with -1 representing perfect negative correlation, 0 representing no connection, and 1 representing perfect positive correlation. The correlation coefficient between Rs and R1, for example, is 0.531, indicating a somewhat good relationship between these two variables. Q1 and n2 have a correlation coefficient of -0.762, indicating a high negative association between both of these variables. It is critical to understand that correlation is not an indication of causality. Correlation just demonstrates a relationship between two variables; it does not imply that one causes the other. Further investigation is required to determine causality.

3. CONCLUSION

The corrosion resistance of 316L stainless steel SS alloys in Hanks' solution (pH 7.4) at 37 °C in the presence of different quantities of the bone drug the mineral calcium hydrogen phosphate shows that the drug acts as an inhibitor and increases the corrosion resistance of 316L stainless steel by protecting the alloy's surface from the environment's damaging physiological medium. A new, stable, and simple ACCMCPE sensor with remarkable performance was developed on carbon paste modified with chitosan (CS), cellulose (CE), and silver nanoparticles (AgNPs) for the detection of calcium hydrogen phosphate medicine. The coefficient of correlation between two variables is represented by each cell in the matrix. The coefficient of correlation is a statistical significance indicator that is used to measure the amount and direction of a relationship between two variables. The overall Cronbach's Alpha value for the model is 0.505.

REFERENCES

[1]. Essa, Khamis, Parastoo Jamshidi, Ji Zou, Moataz M. Attallah, and Hany Hassanin. "Porosity control in 316L stainless steel using cold and hot isostatic pressing." Materials & Design 138 (2018): 21-29. DOI: https://doi.org/10.1016/j.matdes.2017.10.025

[2]. Verma, Pradeep. "Effective Execution of Mergers and Acquisitions for IT Supply Chain." International Journal of Computer Trends and Technology 70, no. 7 (2022): 8-10.

[3]. U. Midhundev; Harshith. T. N,; M. Ramachandran; Kurinjimalar Ramu, “An Empirical Investigation of Innovation and Technology in Banking” , Recent trends in Management and Commerce 4(2), 2023: 121-129.

[4]. Nasr, Ahmed, Soha Abdel Gawad, and Amany M. Fekry. "A sensor for monitoring the corrosion behavior of orthopedic drug cal-cium hydrogen phosphate on a surgical 316L stainless steel alloy as implant." Journal of Bio-and Tribo-Corrosion 6 (2020): 1-10. DOI: https://doi.org/10.1007/s40735-020-0334-5

[5]. Wang, Ping, Liang Zhao, Jason Liu, Michael D. Weir, Xuedong Zhou, and Hockin HK Xu. "Bone tissue engineering via nanostructured calcium phosphate biomaterials and stem cells." Bone research 2, no. 1 (2014): 1-13. DOI: https://doi.org/10.1038/boneres.2014.17

[6]. Madhusudhan Dasari sreeramulu, “Sensitive Analysis of Natural Language Processing Using for MOORA Method”, Computer Science, Engineering and Technology, 1(1), March 2023, 46-53

[7]. Kosar-Grašić, B., B. Purgarić, and H. Füredi-Milhofer. "Precipitation of calcium phosphates from electrolyte solutions—VI the precipitation diagram of calcium hydrogen phosphate." Journal of Inorganic and Nuclear Chemistry 40, no. 11 (1978): 1877-1880. DOI: https://doi.org/10.1016/0022-1902(78)80246-2

[8]. Spoorthi. S,; Harshith. T. N,; M. Ramachandran; Chandrasekar Raja, “ A Review on Child Safety Monitoring System Based on IOT”, Recent trends in Management and Commerce 4(2), 2023: 130-135.

[9]. Thangaraj, Sheela, Paul Olusegun Bankole, Senthil Kumar Sadasivam, and Varuna Kumarvel. "Biodegradation of Reactive Red 198 by textile effluent adapted microbial strains." Archives of Microbiology 204, no. 1 (2022): 12.

[10]. Bhargavi Gorantla, Sreenath Devineni, “Harnessing AI for Optimized Decision-Making: A COPRAS Analysis”, REST Journal on Data Analytics and Artificial Intelligence, 2(3), 2023, 70-77.

[11]. Azab, Shereen M., and Amany M. Fekry. "A novel electrochemical determination for the anti-osteoporosis drug (alendronate sodi-um) and its application for corrosion monitoring of surgical 316 L SS bone implant." Journal of Alloys and Compounds 717 (2017): 25-30. DOI: https://doi.org/10.1016/j.jallcom.2017.05.016

[12]. Sivaraj, D., and K. Vijayalakshmi. "Novel synthesis of bioactive hydroxyapatite/f-multiwalled carbon nanotube composite coating on 316L SS implant for substantial corrosion resistance and antibacterial activity." Journal of Alloys and Compounds 777 (2019): 1340-1346. DOI: https://doi.org/10.1016/j.jallcom.2018.10.341

[13]. Katta, Pradeep PremKumar, and Rajendran Nalliyan. "Corrosion resistance with self-healing behavior and biocompatibility of Ce incorporated niobium oxide coated 316L SS for orthopedic applications." Surface and Coatings Technology 375 (2019): 715-726. DOI: https://doi.org/10.1016/j.surfcoat.2019.07.042

[14]. Inaganti Rambabu, Yalavarthy Sreekanth, “Innovative Solutions: AI-Enabled Medical Devices and Digital Twin Technology Shaping Future Healthcare”, INTERNATIONAL JOURNAL OF CREATIVE RESEARCH THOUGHTS, 11(12), 2023, e497-e506.

[15]. T. Santhosh; Harshitha. T. N,; Sathiyaraj Chinnasamy; M. Ramachandran, “Adaptive Subgradient Methods for Leadership And Development”, Recent trends in Management and Commerce 4(2) 2023, 101-106.

[16]. Abdelrahman, El-Sayed M., Eid R. Abo-Ezz, Khalid S. Essa, T. M. El-Araby, and Khaled S. Soliman. "A new least-squares mini-mization approach to depth and shape determination from magnetic data." Geophysical Prospecting 55, no. 3 (2007): 433-446. DOI: https://doi.org/10.1111/j.1365-2478.2007.00621.x

[17]. Essa, Khalid S., and Mahmoud Elhussein. "A new approach for the interpretation of magnetic data by a 2-D dipping dike." Journal of Applied Geophysics 136 (2017): 431-443. DOI: https://doi.org/10.1016/j.jappgeo.2016.11.022

[18]. Essa, Khalid S., and Mahmoud Elhussein. "A new approach for the interpretation of self-potential data by 2-D inclined plate." Journal of Applied Geophysics 136 (2017): 455-461. DOI: https://doi.org/10.1016/j.jappgeo.2016.11.019

[19]. Shehata, M., S. M. Azab, A. M. Fekry, and M. A. Ameer. "Nano-TiO2 modified carbon paste sensor for electrochemical nicotine detection using anionic surfactant." Biosensors and Bioelectronics 79 (2016): 589-592.

[20]. Bhargavi Gorantla, Sreenath Devineni, “Evaluation of User Experience (UX) Design for Emerging Technologies”, Computer Science, Engineering and Technology, 1(3), 2023, 39-47

[21]. Madhusudhan Dasari sreeramulu, “Optimizing Cloud Computing Networks in Information Security Controls using COPRAS Method”, Computer Science, Engineering and Technology 1(2), 2023, 42-54.
[22]. Heakal, F. El-Taib, A. M. Fekry, and M. Abd El-Barr Jibril. "Electrochemical behaviour of the Mg alloy AZ91D in borate solu-tions." Corrosion science 53, no. 4 (2011): 1174-1185. DOI: https://doi.org/10.1016/j.bios.2015.12.090
[23]. Senthil Kumar Sadasivam Baby Jooju , Sheela Thangaraj, “Degradation Potential of Scedosporium apiospermum SKF2 against an Azo Dye, Reactive Red 180 and Its Phytotoxicity Evaluation”, Applied Ecology and Environmental Sciences, 10 (6), 2022, 388-393
[24]. Ghoneim, A. A., A. M. Fekry, and M. A. Ameer. "Electrochemical behavior of magnesium alloys as biodegradable materials in Hank's solution." Electrochimica Acta 55, no. 20 (2010): 6028-6035. DOI: https://doi.org/10.1016/j.electacta.2010.05.062
[25]. Fekry, A. M., and Rabab M. El-Sherif. "Electrochemical corrosion behavior of magnesium and titanium alloys in simulated body fluid." Electrochimica Acta 54, no. 28 (2009): 7280-7285. DOI: https://doi.org/10.1016/j.electacta.2009.07.047
[26]. Krishnamaneni, Mr Ramesh, and A. N. Murthy. "Advancing Drug Dealing Detection Using Neural Embedding and Nearest Neighbour Searching Techniques." International Journal on Recent and Innovation Trends in Computing and Communication 9, no. 7 (2021): 19-23.
[27]. Bharani, Neha. "Software Quality Measurement using Complexity Analysis of Various Software Engineering Phases." 2020.
[28]. Fekry, Amany M., and Shereen M. Azab. "The development of an innovative nano-coating on the surgical 316 L SS implant and studying the enhancement of corrosion resistance by electrochemical methods using Ibandronate drug." Nano-Structures & Nano-Objects 21 (2020): 100411. DOI: https://doi.org/10.1016/j.nanoso.2019.100411
[29]. Richardson, Sara, and Lo Gorton. "Characterisation of the substituent distribution in starch and cellulose derivatives." Analytica Chimica Acta 497, no. 1-2 (2003): 27-65. DOI: https://doi.org/10.1016/j.aca.2003.08.005
[30]. Krishnamaneni, Ramesh, A. N. Murthy, and S. Sen. "A comparative study of big data mining algorithms for early detection of heart attack risk factors in electronic medical records." International Journal of Computer Engineering and Technology (IJCET) 10, no. 6 (2019): 139-154.
[31]. Inaganti Rambabu, “Preserving Patient Privacy: A Focus on Cyber Security in Healthcare”, International Journal of Emerging Technologies and Innovative Research, 10(10), d218-d222.
[32]. Verma, Pradeep. "Sales of Medical Devices–SAP Supply Chain." International Journal of Computer Trends and Technology 70, no. 9 (2022): 6-12.
[33]. El-Taib Heakal, Fakiha, Amany Mohammed Fekry, and Mohammed Ziad Fatayerji. "Electrochemical behavior of AZ91D magne-sium alloy in phosphate medium—part I. Effect of pH." Journal of applied electrochemistry 39 (2009): 583-591. DOI: https://doi.org/10.1007/s10800-008-9696-y
[34]. Indumathi, M. P., K. Saral Sarojini, and G. R. Rajarajeswari. "Antimicrobial and biodegradable chitosan/cellulose acetate phthalate/ZnO nano composite films with optimal oxygen permeability and hydrophobicity for extending the shelf life of black grapefruits." International journal of biological macromolecules 132 (2019): 1112-1120. DOI: https://doi.org/10.1016/j.ijbiomac.2019.03.171.
[35]. Madhusudhan Dasari sreeramulu, “Analysis of Wireless Security and Networks using COPRAS Method” REST Journal on Data Analytics and Artificial Intelligence 2(4), December 2023, 32-41.
[36]. Bharani, Neha, and Abhay Kothari. "Tools for analysis of various static software complexities for mat lab code." *Turkish Online Journal of Qualitative Inquiry* 12, no. 6 (2021).
[37]. Sreenath Devineni, Bhargavi Gorantla, “Security and Privacy Issues in Internet of Things (IoT) Devices Using COPRAS Method” REST Journal on Data Analytics and Artificial Intelligence, 2(4), 2023, 15-22.